Eur. Phys. J. B **18**, 263–273 (2000)

THE EUROPEAN PHYSICAL JOURNAL B

EDP Sciences

Néel ordered versus quantum disordered behavior in doped spin-Peierls and Haldane gap systems

R. Mélin[a]

Centre de Recherches sur les Très Basses Températures (CRTBT)[b], CNRS BP 166X, 38042 Grenoble Cedex, France
and
Laboratoire de Physique[c], École Normale Supérieure de Lyon, 46 allée d'Italie, 69364 Lyon Cedex 07, France

Received 13 June 2000 and Received in final form 26 August 2000

Abstract. I consider a theoretical description of recent experiments on doping the spin-Peierls compound $CuGeO_3$ and the Haldane gap compounds $PbNi_2V_2O_8$ and Y_2BaNiO_5. The effective theory is the one of randomly distributed spin-1/2 moments interacting with an exchange decaying exponentially with distance. The model has two phases in the (doping, interchain coupling) plane: (i) a Néel ordered phase at small doping; (ii) a quantum disordered phase at larger doping and small interchain interactions. The spin-Peierls compound $CuGeO_3$ and the Haldane gap nickel oxides $PbNi_2V_2O_8$ and Y_2BaNiO_5 fit well into this phase diagram. At small temperature, the Néel phase is found to be reentrant into the quantum disordered region. The Néel transition relevant for $CuGeO_3$ and $PbNi_2V_2O_8$ can be described in terms of a classical disordered model. A simplified version of this model is introduced, and is solved on a hierarchical lattice structure, which allows to discuss the renormalization group flow of the model. It is found that the system looks non disordered at large scale, which is not against available susceptibility experiments. In the quantum disordered regime relevant for Y_2BaNiO_5, the two spin model and the cluster RG in the 1D regime show a power law susceptibility, in agreement with recent experiments on Y_2BaNiO_5. It is found that there is a succession of two distinct quantum disordered phases as the temperature is decreased. The classical disordered model of the doped spin-1 chain contains already a physics relevant to the quantum disordered phase.

PACS. 75.10.Jm Quantized spin models – 75.50.Ee Antiferromagnetics

1 Introduction

Doping quasi-one-dimensional (1D) antiferromagnets with a spin gap has become experimentally possible since the discovery of several inorganic quasi 1D oxides. One of these compounds is $CuGeO_3$ having a spin-Peierls transition at $T_{SP} \simeq 14$ K [1]. Below T_{SP}, the spin-phonon coupling induces a dimerization of the lattice, and the opening of a gap in the spin excitation spectrum. The Haldane gap in spin-1 chains is another example of a spin gap state in low dimensional magnets [2]. Two inorganic spin-1 Haldane gap antiferromagnets have been discovered in the recent years: (i) $PbNi_2V_2O_8$ having a spin gap $\simeq 28$ K [3]. (ii) Y_2BaNiO_5 having a spin gap $\simeq 100$ K [4]. The spin-Peierls compound $CuGeO_3$ and the two nickel oxides $PbNi_2V_2O_8$ and Y_2BaNiO_5 can be doped in a very controlled fashion. Substituting the magnetic Cu sites (having $S = 1/2$) of the spin-Peierls compound $CuGeO_3$ with a variety of ions (Ni [5] – a spin-1 ion –, Co [6] – a spin-3/2 ion –, Zn [7–11] or Mg [12] – non magnetic ions –), or substituting the Ge sites with Si [13] leads to the formation of an antiferromagnetic phase (AF) at low temperature. Moreover, in $CuGeO_3$, there is AF long range order even with an extremely weak concentration of Zn impurities [14]. On the other hand, the two nickel oxides $PbNi_2V_2O_8$ and Y_2BaNiO_5 have been the subject of an important experimental interest recently. It has been shown that substituting the spin-1 Ni sites of the $PbNi_2V_2O_8$ compound with Mg – a spin-0 ion – leads to AF long range order. In the Y_2BaNiO_5 compound, the Ni sites can be substituted with Zn or Mg – non magnetic ions –. In this case, no sign of AF long range order has been reported, even at extremely low temperature [15–17]. Instead, it has been found that the susceptibility has a power-law temperature dependence [18]. Experiments therefore show that doping quasi 1D antiferromagnets with a spin gap can lead to very different situations: either antiferromagnetism, or a power-law susceptibility without AF ordering. The purpose of the present article is to describe these experimental observations in a unified theoretical framework, and provide a detailed theoretical analysis of the different phases of the model.

[a] e-mail: melin@polycnrs-gre.fr
[b] UPR 5001 du CNRS, associated with Université Joseph Fourier
[c] UMR CNRS 5672

On the theoretical side, a lot of efforts have been devoted to understand the behavior of random spin chains. The theoretical tool usually used to study these models is the cluster renormalization group (RG) [19], which is a perturbation theory in the inverse of the strength of the strongest exchange in the chain, and leads to a certain number of exact results at low temperature because the exchange distribution becomes extremely broad. A lot of different models have been solved using this approach. For instance: the Ising chain in a transverse magnetic field [20], the random spin-1/2 chain [21], the spin-1/2 chain with random ferromagnetic and antiferromagnetic bonds [22], the dimerized chain with random bonds [23], the disordered Haldane gap chain [24,25]. These studies have revealed that 1D disordered magnets can be controlled by several types of Griffiths phases: (i) the random singlet phase with a diverging susceptibility and algebraic correlation; (ii) the "weakly disordered" phase with a diverging susceptibility and short range correlations.

An important question is to understand the relation between the available experiments on quasi-one-dimensional oxides and the available theories of disordered 1D magnets. This type of approach followed in the present article incorporates realistic constraints such as interchain couplings and a finite temperature.

The starting point of such our description has been already established in previous works [26–30]. In the doped spin-Peierls systems, non magnetic impurities generate solitonic spin-1/2 degrees of freedom distributed at random with a concentration x. The solitons are confined close to the impurities because of interchain interactions [30–37], and interact with the Hamiltonian

$$\mathcal{H} = \sum_{\langle i,j \rangle} J_{i,j} \mathbf{S}_i \cdot \mathbf{S}_j. \quad (1)$$

The exchange between two spin-1/2 moments at positions (x_i, y_i) and (x_j, y_j) is mediated by virtual excitations of the gaped medium and therefore decays exponentially with distance:

$$J_{i,j} = (-)^{x_i - x_j + y_i - y_j} \times \Delta \exp\left(-\sqrt{\left(\frac{x_i - x_j}{\xi_x}\right)^2 + \left(\frac{y_i - y_j}{\xi_y}\right)^2} \right), \quad (2)$$

where ξ_x and ξ_y are the correlation lengths in the direction of the chains and perpendicular to the chains respectively [28–30]. The form (2) of the exchange incorporates a correlation length in the transverse direction shorter than in the longitudinal direction ($\xi_y = \xi_x/10$, and $\xi_x \simeq 10$ in $CuGeO_3$ [38,39]). The exchange equation (2) is staggered because the dimerized pattern propagates staggered antiferromagnetic correlations. The Hamiltonian (1, 2) is therefore strongly disordered but unfrustrated.

Now, the model relevant to describe doping in a Haldane gap system is almost identical. It is well known that an impurity in a Haldane gap chain generates two "edge" spin-1/2 moments: one at the right and one at the left of the impurity site [40–42]. The spin-1 chain can be thought in terms of a Valence Bond Solid (VBS) [43]. Introducing a paramagnetic site breaks two VBS bonds, therefore resulting in two "edge" spin-1/2 moments. At energies far below the Haldane gap, only these edge moments are the relevant degrees of freedom (see Fig. 1). The two edge moments in the same unit (*i.e.* generated by the same impurity) interact with a ferromagnetic exchange $-J_2$ originating from the coupling to neighboring chains, with therefore the same order of magnitude as the interchain interaction: $J_2 \sim J_\perp$ [44]. The edge moments belonging to different units are coupled by the staggered exchange equation (2).

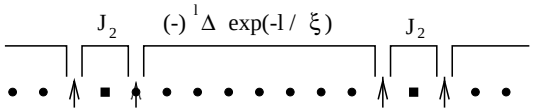

Fig. 1. The low energy effective model of the doped spin-1 system. A paramagnetic impurity (square symbols) generates a unit of two edge moments. The edge moments originating from the same impurity are coupled ferromagnetically by an exchange $-J_2$ having the same order of magnitude as the interchain coupling. Two edge moment at a distance l are coupled by the exchange $(-)^l \Delta \exp(-l/\xi)$.

We find that, depending on the doping concentration and interchain interactions, the model (1, 2) has two regimes: a Néel ordered region and a quantum disordered region. In the Néel ordered region, relevant for $CuGeO_3$ and $PbNi_2V_2O_8$, quantum mechanics plays little role, and we are lead to replace the spin variables in equations (1, 2) by classical Ising spins. We propose here that this type of disordered Ising model is equivalent to another type of disordered Ising model, and solve the hierarchical lattice version of the latter. Using this treatment, we can compute the renormalized exchange distribution. In spite of a strongly disordered initial Hamiltonian (see Eqs. (1, 2)), we find that at large scale, the problem behaves as if it were non disordered. This appears to be consistent with susceptibility experiments showing a well-defined transition even with a small doping concentration [14].

In the quantum disordered region of the phase diagram, the physics is dominated by the formation of randomly distributed singlets. We show that the susceptibility has a power-law behavior, which turns out to be in agreement with existing experiments on Y_2BaNiO_5 [18]. We also find the existence of two distinct "quantum disordered" phases. The high temperature "quantum disordered" phase appears to have been observed experimentally in Y_2BaNiO_5 [18]. There appears to be another low temperature "quantum disordered" phase in which the edge spins in the same unit (see Fig. 1) are frozen into spin-1 objects. Finally, we show that even in the quantum disordered regime of the model, part of the quantum disordered behavior is already contained in the classical disordered magnet.

The article is organized as follows: the phases of the model (1, 2) are discussed in Section 2. We show the existence of two phases: a Néel ordered region and a quantum

disordered region. The nature of these two phases is next discussed in details in Sections 3 and 4. Concluding remarks are given in Section 5.

2 Phases of the model

In this section, we use a phenomenological approach to derive the phase diagram of the model. The calculation of the relevant energy scales in the problem is based on the analysis of a two-spin model. There is a first temperature scale (being a fraction of the spin gap Δ) below which magnetic correlations start to develop inside the chains. There is a second energy scale $T_{\rm typ}$, equal to the typical exchange, associated to singlet formation. There is a third energy scale $T_{\rm Stoner}$ associated to long range AF ordering. The behavior of the model depends strongly on whether $T_{\rm Stoner}$ is larger or smaller than $T_{\rm typ}$.

2.1 Onset of magnetic correlations

Magnetic correlations start to appear inside the chains when the temperature is a fraction of the spin gap Δ. To show this, let us consider a simple model in which two spins at a distance l are coupled antiferromagnetically: $\mathcal{H} = J(l)\mathbf{S}_1 \cdot \mathbf{S}_2$. We use an exchange decaying exponentially with distance (see Eq. (2)): $J(l) = \Delta \exp(-l/\xi)$, and a Poisson bond length distribution $\mathcal{P}(l) = x \exp(-xl)$. Rigorously, the spacing l is a discrete quantity, distributed according to a geometrical distribution. However, the physics will turn out to be controlled by the large-l behavior and it is legitimate to consider l as a continuous variable, and replace the geometrical distribution by the Poisson distribution.

The internal energy of the two-spin model reads

$$U(T) = -\frac{3}{4} x\xi \Delta^{-x\xi} T^{x\xi+1} \times \int_0^{\beta\Delta} u^{x\xi} \frac{\exp(3u/4) - \exp(-u/4)}{\exp(3u/4) + 3\exp(-u/4)} {\rm d}u. \quad (3)$$

This expression can be expanded in T:

$$U(T) \simeq -\frac{3}{4}\frac{x\xi\Delta}{1+x\xi} + \frac{9}{2} x\xi \left(\frac{T}{\Delta}\right)^{x\xi} T + ... \quad (4)$$

Magnetic correlations start to appear in the two-spin model in the low temperature regime in which $U(T)$ is linear in T. This regime appears when T is a fraction of Δ (see Fig. 2).

2.2 Singlet formation

To discuss in what temperature range is the physics controlled by the quantum mechanical ground state (being a singlet), we need to calculate the probability $\mathcal{P}_s(T)$ to find the two spins in a singlet state at a finite temperature $T = 1/\beta$. We have

$$\mathcal{P}_s(T) = \int {\rm d}l\, \mathcal{P}(l) \frac{\exp[3\beta J(l)/4]}{\exp[3\beta J(l)/4] + 3\exp[-\beta J(l)/4]} \quad (5)$$

$$= 1 - 3x\xi \left(\frac{T}{\Delta}\right)^{x\xi} \times \int_0^{\beta\Delta} u^{-1+x\xi} \frac{\exp(-u/4)}{\exp(3u/4) + 3\exp(-u/4)} {\rm d}u, \quad (6)$$

where we used the dimensionless parameter $u = \beta J$. The integral in equation (6) is dominated by the small exchanges and we have $\mathcal{P}_s(T) \simeq 1 - \kappa(T/\Delta)^{x\xi}$, with κ a numerical factor. We are lead to conclude that the ground state occupancy is close to unity below the energy scale $T_{\rm typ} \sim \Delta \exp(-1/(x\xi))$. $T_{\rm typ}$ is nothing but the typical exchange, already identified in a previous work on the 1D model [26,27].

The calculation of the ground state occupancy can be made even simpler by noticing that only the disorder configurations in which the exchange is larger than $\sim T$ are in a singlet configuration. This leads to

$$\mathcal{P}_s(T) \simeq \int_0^{\xi \ln(\beta\Delta)} x \exp(-xl) {\rm d}l \simeq 1 - \left(\frac{T}{\Delta}\right)^{x\xi}.$$

It is remarkable that the energy scale $T_{\rm typ}$ arising from the two-spin model is *identical* to the one obtained previously from the exact solution of the 1D effective model of the spin-Peierls chain [27]. This shows that a model with only two spins contains already the relevant physics.

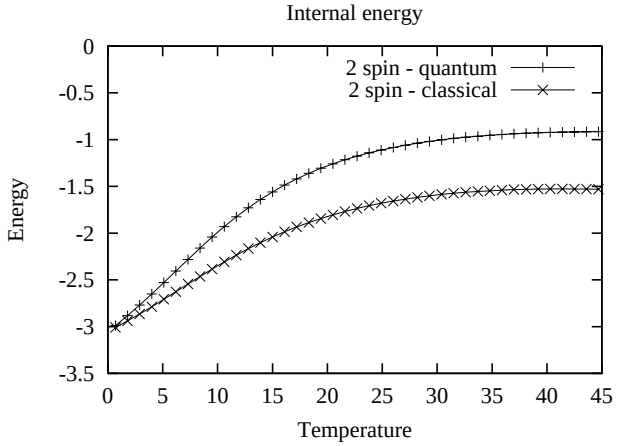

Fig. 2. Temperature dependence of the internal energy of the classical and quantum two-spin model, with $\Delta = 44.7$ K, $\xi = 10$, $x = 0.01$, relevant for $CuGeO_3$. The temperature and energy are calculated in Kelvin. In the two-spin classical model, we considered two spins coupled by an Ising term $\mathcal{H} = (J/2)\sigma_1\sigma_2$.

2.3 Néel ordered versus quantum disordered behavior

At low temperature, correlations between the chains induce a long range ordering of the spin system. The simplest phenomenological description of long range ordering

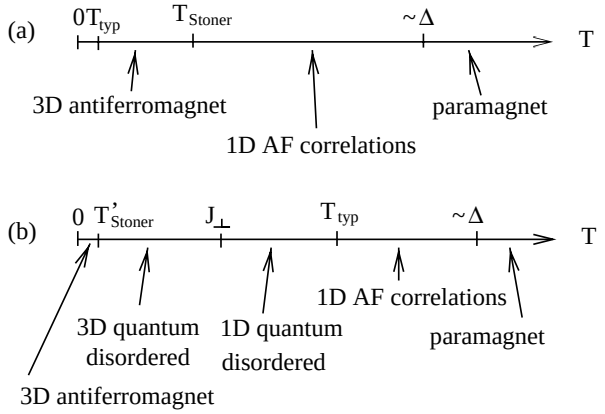

Fig. 3. In the models with 3D antiferromagnetism (a) $T_{\rm typ}$ is far below $T_{\rm Stoner} = J_\perp x\xi$, with therefore a classical transition to an AF phase. This is the case for $PbNi_2V_2O_8$ as well as $CuGeO_3$. In the models with a quantum disordered ground state (b), $J_\perp$ is far below $T_{\rm typ}$, which occurs in Y_2BaNiO_5. In this case, the classical paramagnet has a cross-over to a 1D quantum disordered state with formation of random singlets. Below $J_\perp$, singlets are formed among spins belonging to different chains. Below $T'_{\rm Stoner}$, there is a transition to a reentrant antiferromagnetic phase. Intrachain correlations start to play a role when the temperature is below a fraction of the spin gap Δ.

is provided by a Stoner model, already considered in reference [28]. In $CuGeO_3$, there is a succession of three regimes (see Fig. 3a): (i) a paramagnet at high temperature, (ii) intrachain correlations develop when the temperature is a fraction of Δ (iii) interchain correlations give rise to long range antiferromagnetism below $T_{\rm Stoner} = J_\perp x\xi$.

In $PbNi_2V_2O_8$, the relevant parameters are $\Delta \simeq 30$ K, $x \simeq 0.02$, $J_\perp \simeq 1.1$ K. We approximate the correlation length in the Haldane gap phase to be $\xi \simeq 6$. The true correlation length is expected to be larger than this value because $PbNi_2V_2O_8$ is close to a transition to an Ising ordered antiferromagnet [3]. We find $T_{\rm Stoner} = 0.13$ K, $T_{\rm typ} = 6$ mK, showing that the same succession of regimes occur in $PbNi_2V_2O_8$ and $CuGeO_3$ (see Fig. 3a). This is compatible with existing experiments in $PbNi_2V_2O_8$ [3].

Therefore, in $CuGeO_3$ and $PbNi_2V_2O_8$, one has $T_{\rm Stoner} \gg T_{\rm typ}$. This implies that singlet formation plays little role in the physics of the antiferromagnetic transition. The quantum two-spin model can then be well mimicked by the *classical* two-spin model. For instance, the internal energy of the classical and quantum two-spin models have an identical temperature dependence (see Fig. 2). This indicates that one might expect to obtain a reasonable description of antiferromagnetism in $CuGeO_3$ and $PbNi_2V_2O_8$ on the basis of a classical model, which we analyze in details in Section 3.

Now, the situation is different in Y_2BaNiO_5, where one has $\Delta \simeq 100$ K, $\xi \simeq 6$, $J_\perp \simeq 0.3$ K, and $x \simeq 0.04$ [18]. We find $T_{\rm typ} = 1.6$ K, and $T_{\rm Stoner} = 0.07$ K. What is new compared to $CuGeO_3$ and $PbNi_2V_2O_8$ is that a well defined quantum disordered regime is present below $T_{\rm typ}$. In between $J_\perp$ and $T_{\rm typ}$, there is singlet formation in the chain direction, and below $J_\perp$, the singlets develop in the transverse direction. Below the energy scale $T_{\rm typ}$, the staggered susceptibility is well described by the one of the random spin-1 chain [24,25]

$$\chi(T) \sim xT^{\alpha-1}/T_{\rm typ}^{\alpha}. \tag{7}$$

Using a cluster RG calculation, we will calculate the susceptibility in section 4.2 and show that it has indeed a power-law temperature dependence. The Stoner criterion leads to the ordering temperature

$$\frac{T'_{\rm Stoner}}{T_{\rm typ}} = \left(\frac{J_\perp x\xi}{T_{\rm typ}}\right)^{1/(1-\alpha)}.$$

This shows that the quantum disordered model transits to a reentrant antiferromagnetic ground state below $T'_{\rm Stoner}$. The different regimes of the model are shown in Figure 3b.

The existence of two classes of models is best summarized by calculating the ratio

$$\frac{T_{\rm Stoner}}{T_{\rm typ}} = \frac{J_\perp}{\Delta} x\xi {\rm e}^{1/(x\xi)},$$

which can be smaller or larger than unity, controlling whether the model has a Néel transition at $T_{\rm Stoner}$ or is in a quantum disordered regime. These two behaviors, as well as a comparison between the model and existing experiments on $CuGeO_3$, $PbNi_2V_2O_8$ and Y_2BaNiO_5, have been reported on the phase diagram in Figure 4.

3 Nature of the antiferromagnetic transition

3.1 Motivation of the hierarchical lattice study

In low doping experiments in $CuGeO_3$, Manabe *et al.* have measured the doping dependence of the Néel temperature, and found that the experimental data in the range $x > 0.1\%$ could be well fitted by the behavior $T_{\rm N} \sim A\exp(-B/x)$ [14]. This suggests that there is no critical concentration associated to antiferromagnetism. As already pointed out in references [28,29], the model (1, 2) shows sings of compatibility with these experiments. The main unsolved question raised by the experiments by Manabe *et al.* [14] is to determine whether the maximum in the susceptibility is really the signature of an antiferromagnetic phase transition with a diverging staggered correlation length. In fact, the susceptibility experiments give no information about the existence / absence of a diverging correlation length, and there are are no neutron experiments with a concentration of impurities of order $\simeq 0.1\%$. On the theoretical side, we used previously several approaches to describe the nature of the antiferromagnetic phase of the model (1, 2): a Stoner model [28], a decimation method, a cluster RG [29], and a Bethe-Peierls solution of the classical model [29]. It appears that different treatments of the model have lead

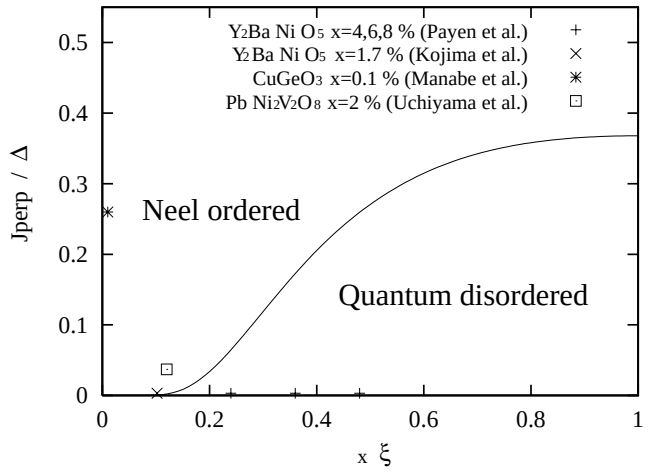

Fig. 4. Phase diagram in the plane $(x\xi, J_\perp/\Delta)$. The solid line is $J_\perp/\Delta = 1/(x\xi)\exp[-1/(x\xi)]$, delimitating the transition from the Néel ordered region to the quantum disordered region. Various experimental systems have been reported on the diagram: (+, ×) Y_2BaNiO_5 [17,18] (being quantum disordered); (*) $CuGeO_3$ [14] (being antiferromagnetic); (□) $PbNi_2V_2O_8$ [3] (being antiferromagnetic). The values of $J_\perp$ and ξ have been taken from these references. This phase diagram is valid above the temperature scale $T'_{\rm Stoner}$. Below $T'_{\rm Stoner}$, the antiferromagnet is reentrant inside the quantum disordered phase.

to different answers. For instance, there is a well defined transition in the Stoner criterion and the Bethe-Peierls treatments [28,29]. On the contrary, there is no transition in the decimation method where the Hamiltonian (1, 2) is mapped onto a percolation model [28]. A possible approach to this problem would be to generalize the work in reference [45]: instead of considering the model (1, 2) with infinite range exponential interactions, it is possible to approximate the problem by considering the Voronoi lattice model with exponential interactions, in which each lattice site has a finite number of neighbors. This model is well suited for carrying out numerical simulations, and avoids the difficulty that the initial model (1, 2) has infinite range interactions.

Here, we would like to follow a different route and replace the original Hamiltonian (1, 2) by a simplified one. This is done by noticing that the essential feature of the Hamiltonian (1, 2) is that the exchange between two spins at a random position is distributed according to

$$\mathcal{P}(J) = \frac{x\xi}{\Delta}\left(\frac{J}{\Delta}\right)^{x\xi-1}, \qquad (8)$$

where we used the spacing distribution $P(l) = x\exp(-xl)$ and the exchange $J(l) = \Delta\exp(-l/\xi)$. We replace the original model (1, 2) by another model in which the spins are on the sites of a regular square lattice, and have a random nearest neighbor exchange in the distribution (8). Because the square lattice model with the exchange distribution (8) and the original model (1, 2) are controlled by the same type of disorder, it is natural to conjecture that the two models have an identical physics. One way

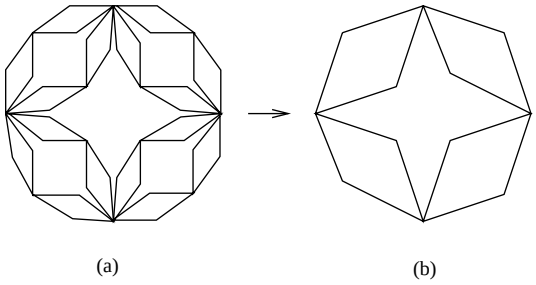

Fig. 5. The hierarchical diamond used in the Migdal-Kadanoff renormalization. (a) A hierarchical lattice with 3 generations. (b) A hierarchical lattice with 2 generations. One RG transformation consists in decimating the sites at the deepest into the lattice, *i.e.* for instance transforming the lattice (a) into the lattice (b).

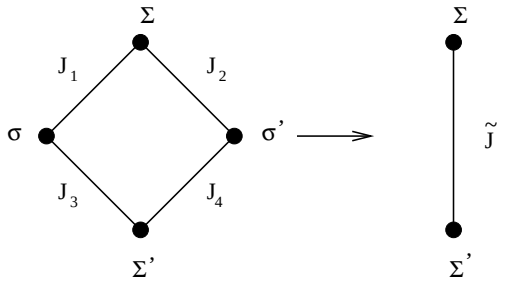

Fig. 6. The notations used in the renormalization.

to study the square lattice model with the exchange distribution (8) would be to perform large scale Monte Carlo simulations. There is however a more direct way to handle the model, which consists in replacing the square lattice by a recursive hierarchical lattice (see Fig. 5), where the Migdal Kadanoff RG equations can be obtained in an exact form. We will show that a non trivial physics is going on in the hierarchical lattice model, which is an indication there is also a non trivial physics in the square lattice model with the exchange distribution (8).

3.2 Renormalization group equations

Let us derive the RG equations of the Ising model with the exchange distribution (8) on a hierarchical lattice. The partition function associated to the exchange configuration in Figure 6a reads

$$Z(\Sigma,\Sigma') = \sum_{\sigma,\sigma'} \exp\beta\left[J_1\Sigma\sigma + J_2\Sigma\sigma' + J_3\Sigma'\sigma + J_4\Sigma'\sigma'\right], \qquad (9)$$

and we impose that equation (9) be identical to the partition function associated to the exchange configuration in Figure 6b, up to a proportionality factor:

$$Z(\Sigma,\Sigma') = \mathcal{N}\exp(\beta\tilde{J}\Sigma\Sigma').$$

Using the relation

$$\tilde{J} = \frac{1}{2\beta} \ln \left[\frac{Z(+,+)}{Z(+,-)} \right],$$

we find $\tilde{J} = \tilde{J}_{1-3} + \tilde{J}_{2-4}$, where

$$\tilde{J}_{1-3} = \frac{1}{2\beta} \ln \left[\frac{\cosh\left(\beta(J_1 + J_3)\right)}{\cosh\left(\beta(J_1 - J_3)\right)} \right],$$
$$\tilde{J}_{2-4} = \frac{1}{2\beta} \ln \left[\frac{\cosh\left(\beta(J_2 + J_4)\right)}{\cosh\left(\beta(J_2 - J_4)\right)} \right]. \quad (10)$$

Now that we have determined the renormalization of the exchanges, we iterate the exchange distribution. Noting $P(J_1)$ ... $P(J_4)$ the distribution of the exchanges J_1 ... J_4, and $P(\tilde{J})$ the distribution of the renormalized exchange $\tilde{J}$, we have

$$\tilde{P}(\tilde{J}) = \int \mathrm{d}J_1 \mathrm{d}J_2 \mathrm{d}J_3 \mathrm{d}J_4 \, P(J_1)P(J_2)P(J_3)P(J_4)\delta \times \left[\tilde{J} - \tilde{J}_{1-3} - \tilde{J}_{2-4} \right]. \quad (11)$$

It will be useful to change variables to the bond lengths $l = \xi \ln(\Delta/J)$ and iterate the bond length distribution $p(l)$ instead of the exchange distribution $P(J)$.

To calculate numerically the iteration of the exchange distribution (11), we use a discrete bond length $l = 1, ..., N$, and we introduce an upper cut-off for the bond length. This is valid if we can check that the RG flow does not depend on N.

3.3 Analysis of the RG flow

The RG flow of the model is shown in Figure 7. We have shown in this figure the evolution of the average bond length $\langle\langle l \rangle\rangle$ and the width of the bond length distribution $\sqrt{\langle\langle (l - \langle\langle l \rangle\rangle)^2 \rangle\rangle}$. At low temperature, the average bond length renormalizes to zero (ordered phase) while at high temperature it renormalizes to infinity (paramagnetic phase). Therefore, there is a well-defined transition in the model. We have checked that the transition temperature is independent on the cut-off N used to iterate the bond length distribution. The existence of a thermodynamic transition could have been anticipated on the basis of the simplest possible approximation of the RG flow (see Appendix A). What is less obvious is that, after a transient in the first RG iterations, the width of the exchange distribution becomes much smaller than the average exchange: in spite of a broad initial exchange distribution in which $\langle\langle l \rangle\rangle = \sqrt{\langle\langle (l - \langle\langle l \rangle\rangle)^2 \rangle\rangle}$, the system renormalizes to an almost disorder-free exchange distribution in which $\sqrt{\langle\langle (l - \langle\langle l \rangle\rangle)^2 \rangle\rangle} \ll \langle\langle l \rangle\rangle$. Therefore, at large scale, the spin system looks ordered while inhomogeneities are visible only at small scale. This type of behavior may explain why there is a pronounced maximum in the temperature dependence of the susceptibility even at very low doping [14].

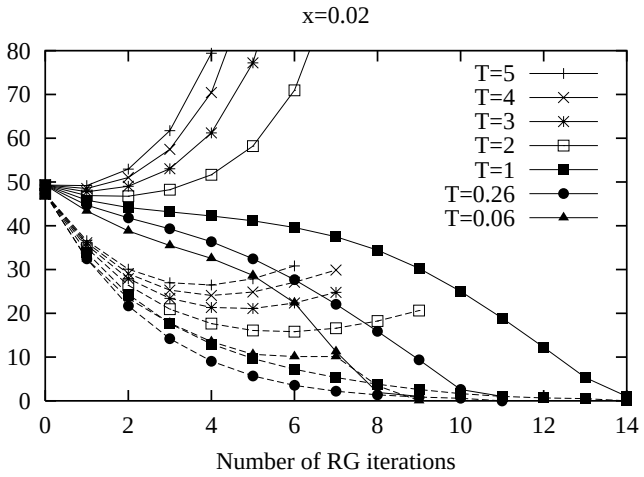

Fig. 7. RG flow of the classical model relevant for the antiferromagnetic transition in $CuGeO_3$. The parameters are $\Delta = 44.7$ K and $\xi = 10$, and we used a cut-off $N = 300$. The doping concentration is $x = 0.02$. The solid line represents the evolution of the average bond length $\langle\langle l \rangle\rangle$. The doted lines represent the evolution of the width of the bond length distribution $\sqrt{\langle\langle (l - \langle\langle l \rangle\rangle)^2 \rangle\rangle}$. The RG trajectories with $T = 5$ (+), $T = 4$ (×), $T = 3$ (*) and $T = 2$ (□) flow into the paramagnetic phase (the bond length renormalizes to infinity). The trajectories with $T = 1$ (■), $T = 0.26$ (•), $T = 0.06$ (▲) flow into the ferromagnetic phase (the bond length renormalizes to zero).

4 Nature of the quantum disordered region

Now, we would like to investigate the behavior of the model in the quantum disordered region, and compare it to experimental data on the Haldane gap compound Y_2BaNiO_5. More specifically, we would like to determine whether the behavior of the model is compatible with the susceptibility experiments by Payen *et al.* [18], who reported that the susceptibility of Y_2BaNiO_5 has a power-law temperature dependence. In our opinion, it is an important question to determine which ingredients should be incorporated in the theoretical model to describe the existing experiments. A first strategy, followed by Batista *et al.* [46] is to look for the "most realistic possible" model. The first step in this approach is to consider that the relevant Hamiltonian for Y_2BaNiO_5 takes the form

$$\mathcal{H} = \sum_i \left\{ J\mathbf{S}_i \cdot \mathbf{S}_{i+1} + D(S_i^z)^2 + E\left[(S_i^x)^2 - (S_i^y)^2\right] \right\}. \quad (12)$$

The anisotropy parameters in equation (12) have been determined by fitting inelastic neutron scattering experiments [47,48]. Next, a density matrix renormalization group (DMRG) method has been used to treat the Hamiltonian (12) in the presence of magnetic impurities. The authors of reference [46] are then able to reproduce specific heat experiments, and also arrive to an agreement with susceptibility experiments [18]. The main objection

that one might be tempted to formulate is that the Hamiltonian of the spin-1 chain relevant for Y_2BaNiO_5 contains already three adjustable parameters, and that two more additional gyromagnetic factors have been added to describe the susceptibility experiments [18]. Here, it is proposed that the power law temperature dependence of the susceptibility is a generic feature of the quantum disordered region of the phase diagram, that can be explained in a model with only a minimal number of ingredients.

4.1 Two-spin model

As we already explained in the Introduction, in the low energy model relevant to describe the doped Haldane gap compound, each paramagnetic impurity generates a unit of two "edge" spin-1/2 moments (see Fig. 1). The two spin-1/2 moments in the same unit are coupled by a ferromagnetic exchange J_2 the magnitude of which is of order of interchain interactions [44]. As shown in Figure 1, there is a staggered exchange $(-)^l \exp(-l/\xi)$ coupling two edge moments at a distance l.

Let us first consider the simplest model in which the impurities are assumed to cut the chain into finite segments: $J_2 = 0$. This is a valid model if the temperature is larger than J_2, or equivalently, than the strength of interchain interactions. Consider two edge spins at distance l, coupled with a Heisenberg Hamiltonian $\mathcal{H} = J(l)\mathbf{S}_1 \cdot \mathbf{S}_2 - h(\mathbf{S}_1^z + \mathbf{S}_2^z)$, and the exchange $J(l) = \Delta(-)^l \exp(-l/\xi)$, with $\mathcal{P}(l_+) = x \exp(-x l_+)$ the distribution of even length segments and $\mathcal{P}(l_-) = x \exp(-x l_-)$ the distribution of odd length segments. It is easy to calculate the average magnetization in a magnetic field h:

$$\langle\langle M(h,T)\rangle\rangle = \frac{1}{2} x \int_0^{\Delta} \mathcal{P}(J) \times [M_+(h,T,J) + M_-(h,T,J)]\,\mathrm{d}J, \tag{13}$$

with $\mathcal{P}(|J|) = (x\xi/\Delta)(|J|/\Delta)^{-1+x\xi}$ the exchange distribution, and

$$M_+(h,T,J) = \frac{\mathrm{e}^{\beta h} - \mathrm{e}^{-\beta h}}{\mathrm{e}^{\beta h} + \mathrm{e}^{-\beta h} + 1 + \mathrm{e}^{\beta J}},$$
$$M_-(h,T,J) = \frac{\mathrm{e}^{\beta h} - \mathrm{e}^{-\beta h}}{\mathrm{e}^{\beta h} + \mathrm{e}^{-\beta h} + 1 + \mathrm{e}^{-\beta J}} \tag{14}$$

the magnetization of the spins coupled by an antiferromagnetic or ferromagnetic exchange J at a finite temperature $T = 1/\beta$. To calculate the magnetization (13, 14), it is convenient to integrate by parts:

$$\langle\langle M(h,T)\rangle\rangle = xA + x\left(\frac{T}{\Delta}\right)^{x\xi} \int_0^{\Delta/T} u^{x\xi} f(u, h/T), \tag{15}$$

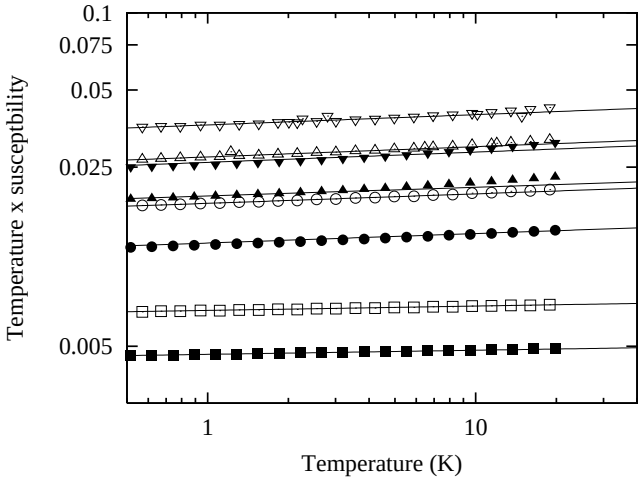

Fig. 8. Log-log plot of the temperature dependence of $T\chi(T)$ for the two-spin model and the cluster RG of the full chain. We used $\Delta = 100$ K, $\xi = 6$. For the two-spin model, we used $x = 0.01$ (□), $x = 0.03$ (⊙), $x = 0.05$ (Δ), $x = 0.07$ (∇). The same symbols filled in black have been used for the cluster RG calculation. The product $T\chi(T)$ has been fitted to a power-law dependence $T\chi(T) \sim T^{\alpha}$, with $\alpha = 0.017$ ($x = 0.01$), $\alpha = 0.037$ ($x = 0.03$), $\alpha = 0.04$ ($x = 0.05$), $\alpha = 0.04$ ($x = 0.07$).

with

$$A = \frac{1}{2}\left[\frac{\mathrm{e}^{\beta h} - \mathrm{e}^{-\beta h}}{\mathrm{e}^{\beta h} + \mathrm{e}^{-\beta h} + 1 + \mathrm{e}^{\Delta/T}} + \frac{\mathrm{e}^{\beta h} - \mathrm{e}^{-\beta h}}{\mathrm{e}^{\beta h} + \mathrm{e}^{-\beta h} + 1 + \mathrm{e}^{-\Delta/T}}\right] \tag{16}$$

$$f(u, \frac{h}{T}) = -\frac{1}{2}\frac{\mathrm{d}}{\mathrm{d}u}\left[\frac{\mathrm{e}^{\beta h} - \mathrm{e}^{-\beta h}}{\mathrm{e}^{\beta h} + \mathrm{e}^{-\beta h} + 1 + \mathrm{e}^{u}} + \frac{\mathrm{e}^{\beta h} - \mathrm{e}^{-\beta h}}{\mathrm{e}^{\beta h} + \mathrm{e}^{-\beta h} + 1 + \mathrm{e}^{-u}}\right]. \tag{17}$$

The resulting susceptibility is shown in Figure 8, where it is visible that the product $T\chi(T) \sim T^{\alpha}$ has a power-law behavior at low temperature, like what has been observed in experiments on Y_2BaNiO_5 [18]. The magnetization in an applied magnetic field is shown in Figure 9, and is close to the experimental observation [18]. This shows that this model with only two spins contains much of the physics as far as the temperature is above the interchain coupling $J_\perp$.

4.2 Cluster RG

4.2.1 Quantum disordered phase I

Now, let us consider the cluster RG of the model with a finite J_2, and first consider the behavior of the model when the temperature is larger than J_2. I refer the reader to references [19,22,29] for an explanation of the method, and just present here the results. First, if the temperature

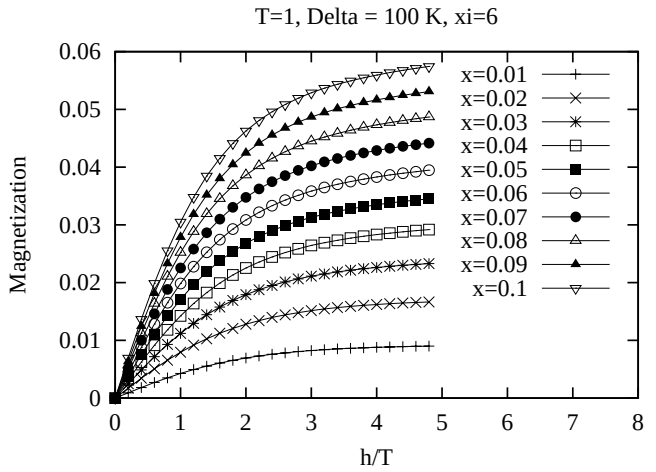

Fig. 9. Magnetization of the two-spin quantum model, with the parameters relevant for Y_2BaNiO_5: $\Delta = 100$ K, $\xi = 6$.

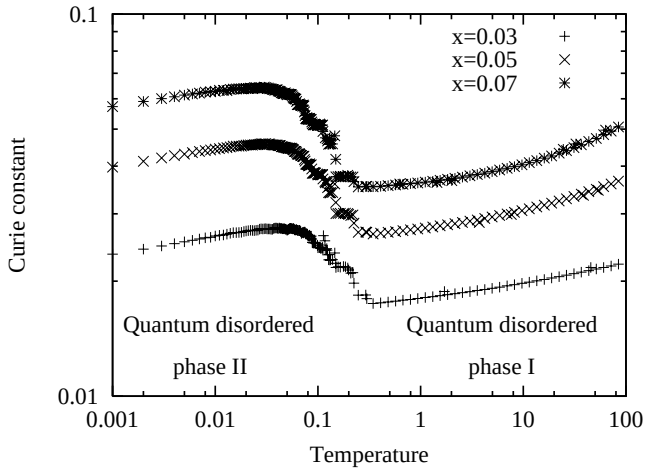

Fig. 10. Temperature dependence of the Curie constant, with the parameters relevant for Y_2BaNiO_5: $\Delta = 100$ K, $\xi = 6$, and $x = 0.03$, $x = 0.05$, and $x = 0.07$. We renormalized a chain with 10 000 sites and averaged over 100 realizations of disorder. We used $J_2 = 0.3$ K.

is above J_2, we find that the exponent of the power-law Curie constant $T\chi(T) \sim T^{\alpha}$ is identical to the one of the two-spin model (see Fig. 8). This is not a surprise because above J_2 the edge moments in the same unit remain uncoupled and the cluster RG contains the same physics as the two-spin model. Moreover, the two-spin model is an exact treatment while the cluster RG is approximate. The agreement between the two methods shows the validity of the cluster RG method.

4.2.2 Quantum disordered phase II

Now, I consider the cluster RG of a single chain at a temperature smaller than $J_2 \sim J_\perp$. The temperature dependence of the Curie constant is shown in Figure 10. It is visible that the Curie constant increases strongly with decreasing the temperature below J_2. This is because when $T \sim J_2$, the survival spin-1/2 moments in the same unit are frozen into spin-1 moments. This phenomenon is not quantum in nature because it occurs also in the classical disordered model, which is analyzed in details below.

Once the freezing into spin-1 units has been done at the energy scale J_2, the resulting effective model is again the one of spin-1 objects with random exchanges, being ferromagnetic or antiferromagnetic. This results in the low temperature quantum disordered phase II in Figure 10.

In the presence of a finite interchain coupling, one still expects the appearance of two types of quantum disordered regions. It is also expected that the quantum disordered phase II in Figure 10 is a 3D random singlet state, with singlet formation between spins belonging to different chains. The cross-over to a 3D regime is however not expected to change the shape of the temperature dependence of the susceptibility (see Fig. 10).

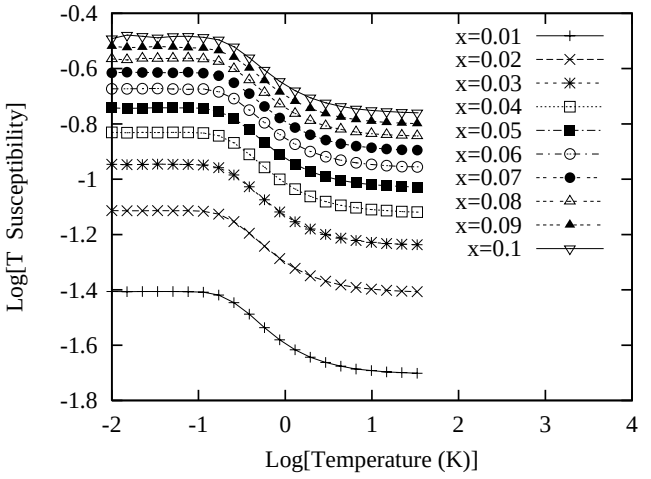

Fig. 11. Temperature dependence of the Curie constant $T\chi(T)$ in the classical analog of the doped spin-1 chain. The parameters are $\xi = 6$, $\Delta = 100$ K, $J_2 = 0.3$ K, relevant for Y_2BaNiO_5. The Curie constant crosses over from $2x$ at high temperature to $4x$ at low temperature.

4.3 Classical disordered model

Now, let us determine to what extend the physics of the classical magnet resembles the physics of the quantum magnet. The Ising chain Hamiltonian reads

$$\mathcal{H} = \sum_i J_{i,i+1}\sigma_i\sigma_{i+1},$$

with the Ising variables σ_i corresponding to the consecutive edge moments, and $J_{i,i+1}$ determined according to the rules in Figure 1. The even bonds correspond to a ferromagnetic exchange $-J_2$ and the odd bonds correspond

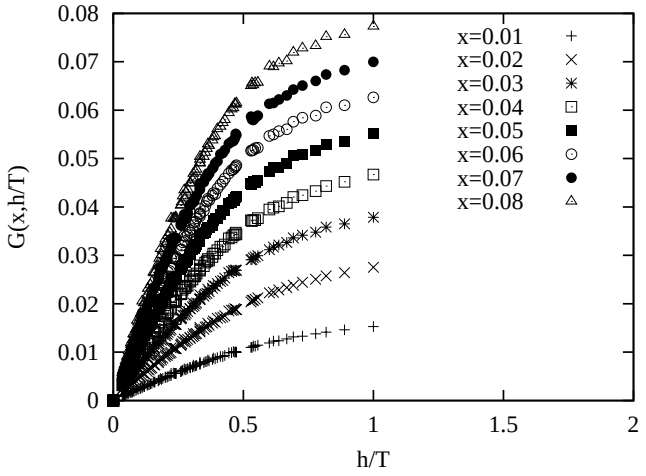

Fig. 12. Scaling of the magnetization $M(h,T) = T^{-\gamma}G(x,h/T)$ in the classical analog of the doped spin-1 chain. We have shown $G(x,h/T)$ as a function of h/T. Each curve corresponds to values of T varying from 0.9 to 3 and h varying from 0 to 1. We used the parameters $\xi = 6$, $\Delta = 100$ K relevant for Y_2BaNiO_5. We used $\gamma \simeq 0.05$.

to an exchange $J(l) = \Delta(-)^l \exp[-l/\xi]$, with the spacing l drawn in the Poisson distribution $P(l) = x\exp(-xl)$.

As shown in Appendix 5, the Curie constant crosses over from $2x$ at high temperature to $4x$ at low temperature, when the temperature decreases below J_2 (see Fig. 11). Therefore, in the classical model, the product $T\chi(T)$ increases monotonically with a decreasing temperature, while the opposite is observed experimentally in Y_2BaNiO_5 [18]. This is not unexpected because the classical model cannot describe the gapless Haldane phases. Nevertheless, the increase in the susceptibility below J_2 is very reminiscent of the behavior of the quantum model in the same temperature range. This is because the freezing of the edge moments of the same unit in a ferromagnetic alignment occurs both in the classical and quantum models.

The scaling function of the magnetization can be calculated easily by iterating numerically the magnetization distribution (20) and using the relation

$$\mathcal{P}(M,h) = \frac{\mathcal{P}(M,h=0)\mathrm{e}^{\beta hM}}{\sum_{M'}\mathcal{P}(M',h=0)\mathrm{e}^{\beta hM'}}$$

to obtain the magnetization distribution in a finite magnetic field. The magnetization takes the form $M(h,T) = T^{-\gamma}G(x,h/T)$ in a given temperature range where the susceptibility can be approximated by $\chi(T) \sim T^{-1-\gamma}$. The scaling function is shown in Figure 12, where it is visible that it has qualitatively the correct behavior in spite of the exponent γ having the wrong sign compared to experiments. Therefore, the shape of the scaling function of the magnetization does not appear to be a crucial test to the model.

5 Conclusions

To conclude, the present work was intended to describe doping a spin-Peierls and a Haldane gap state in a unified framework. We have first shown how the relevant energy scales in the problem could be calculated from the analysis of a two-spin model, which allowed to discuss the phases of the model as a function of the doping concentration and interchain interactions. In the relevant temperature window, there are two distinct regions depending on the doping concentration and interchain interactions: (i) an antiferromagnetic region; (ii) a quantum disordered region. remarkably, this type of phase diagram compares well with the known behavior of the spin-Peierls compound $CuGeO_3$ and the two nickel oxides $PbNi_2V_2O_8$ and Y_2BaNiO_5.

Next, we used our approach to investigate in more details the two possible phases of the model. We have shown that the physics in the antiferromagnetic region of the phase diagram is *classical in nature* and therefore we were lead to study the corresponding Ising model. We have replaced the original Hamiltonian (1, 2) by another Hamiltonian having the same features, and presented the solution of the latter Hamiltonian on a hierarchical lattice structure. Interestingly, we find that the renormalized problem is non disordered. This is in agreement with the presence of a well-defined cusp associated to antiferromagnetism in the susceptibility [14].

In the "quantum disordered" region of the phase diagram, the physics is strongly controlled by quantum fluctuations. Already in a model with two spins only does the susceptibility have a power-law temperature dependence, very similar to the experimental observation [18]. We have suggested that there is no need to introduce many coupling constants to reach an agreement between the model and experiments. Going beyond the level of a two-spin model, we have found the existence of another quantum disordered phase at low temperature. We have analyzed the behavior of the classical model and shown it contains already a physics relevant to the quantum model.

Appendix A: Projection of the RG flow on a trial exchange distribution

We would like to present the simplest possible approximation of the RG equations obtained in Section 3.2 in which we project the RG flow onto the single parameter distribution $p_n(l) = \delta(l - L_n)$. The initial distribution is obtained *via* the relation $\int p_0(l)\mathrm{d}l = \int x\exp(-xl)\mathrm{d}l$, with $p_0(l) = \delta(l - L_0)$. This leads to

$$L_0 = \xi \ln\left(\frac{1+x\xi}{x\xi}\right). \tag{18}$$

Next, we start from the distribution $p_n(l)$, make one RG transformation (11), and impose that the iterated distribution has the same first moment as $p_{n+1}(L)$, from what we can determine the parameter L_{n+1}:

$$L_{n+1} = \xi \ln \frac{\beta\Delta}{\ln\cosh\left[2\beta\Delta\exp\left(-L_n/\xi\right)\right]}\cdot \tag{19}$$

Since we want to discuss the stability of the paramagnetic phase, we consider equation (19) in the limit of a large bond length: $L_{n+1} \simeq -\xi \ln(2\beta\Delta) + 2L_n$. In this limit, we find $L_n = \xi \ln(2\beta\Delta) + (L_0 - \xi \ln(2\beta\Delta))\, 2^n$. Using equation (18), we obtain a phase transition at the temperature

$$T_{\rm c} = \frac{2\Delta x \xi}{1 + x\xi}.$$

The transition temperature is in agreement with what has been found in previous works with different methods (the Stoner criterion [28] and the Bethe-Peierls method [29]). As we show in the body of the article, the renormalized exchange distribution can be well approximated by the distribution $p_n(l) = \delta(l - L_n)$ in the sense that the problem renormalizes to a non disordered one.

Appendix B: Solution of the classical analog of the doped spin-1 chain

We consider a finite chain with N edge moments in which the end spin at site N is frozen in the direction +, and note $\mathcal{P}_N^+(M)$ the corresponding magnetization distribution. We note $x_i = \exp(\beta J_i)/[\exp(\beta J_i) + \exp(-\beta J_i)]$ the probability to find the spins σ_i and σ_{i+1} in an antiparallel alignment. We have

$$\mathcal{P}_{N+1}^+(M) = (1 - x_N)\mathcal{P}_N^+(M-1) + x_N \mathcal{P}_N^-(M-1). \tag{20}$$

Using the relation $\mathcal{P}_N^+(M) = \mathcal{P}_N^-(-M)$, we get

$$\langle M \rangle_{N+1}^+ = (1 - 2x_N)\langle M \rangle_N^+ + 1 \tag{21}$$

$$\langle M^2 \rangle_{N+1} = \langle M^2 \rangle_{N+1} + 2(1 - 2x_N)\langle M \rangle_N^+ + 1. \tag{22}$$

These relations can be solved analytically. For this purpose, let us separate the even bonds coupled by the ferromagnetic exchange $-J_2$ and note $x_{\rm F} = {\rm e}^{-\beta J_2}/[{\rm e}^{\beta J_2} + {\rm e}^{-\beta J_2}]$. The odd bonds are ferromagnetic or antiferromagnetic and we are lead to define

$$y = \sum_{l=1}^{+\infty} \mathcal{P}(l) \frac{{\rm e}^{-\beta J(l)}}{{\rm e}^{\beta J(l)} + {\rm e}^{-\beta J(l)}}.$$

The magnetization of a chain with an even number of sites $N = 2p$ is found to be

$$\langle M \rangle_{2p}^+ = \frac{2(1 - x_{\rm F})}{1 - X}\left[1 - X^p\right], \tag{23}$$

with $X = (1 - 2x_{\rm F})(1 - 2y)$. The correlation length is $\xi_{\rm T} = -2/\ln X$. With an odd number of sites $N = 2p + 1$, the magnetization is

$$\langle M \rangle_{2p+1}^+ = \frac{2(1-y)}{1-X} - \frac{X + 1 - 2y}{1 - X} X^p. \tag{24}$$

The expressions of the first moment (23, 24) are next used to solve for the second moment:

$$\langle M^2 \rangle_{2p} \sim 2p \left\{ 1 + \frac{2(1-2y)(1-x_{\rm F})}{1-X} + \frac{2(1-2x_{\rm F})(1-y)}{1-X} \right\},$$

to leading order in the chain length $2p$. At high temperature, one has $y \sim 1/2$, $x_{\rm F} \sim 1/2$ and $X \sim 0$, and therefore a susceptibility scaling like $\chi \sim 2x/T$. At low temperature, one has $x_{\rm F} \sim 0$, $y \sim 1/2$ and $X \sim 0$, and a susceptibility scaling like $\chi \sim 4x/T$. Therefore, the Curie constant crosses over from the high temperature value $2x$ to $4x$ at low temperature, because the spin-1/2 moments in the same unit are frozen ferromagnetically at a temperature $T \sim J_2$ (see Fig. 11).

References

1. M. Hase, I. Terasaki, K. Uchinokura, Phys. Rev. Lett. **70**, 3651 (1993); J.P. Pouget, L.P. Regnault, M. Ain, B. Hennion, J.P. Renard, P. Veillet, G. Dhalenne, A. Revcolevschi, Phys. Rev. Lett. **72**, 4037 (1994).
2. F.D.M. Haldane, Phys. Lett. A **93**, 464 (1983); Phys. Rev. Lett. **50**, 1153 (1983).
3. Y. Ichiyama, Y. Sasago, I. Tsukuda, K. Uchinokura, A. Zheludev, T. Hayashi, N. Miura, P. Boni, Phys. Rev. Lett. **83**, 632 (1999).
4. D.J. Buttrey, J.D. Sullivan, A.L. Rheingold, J. Solid. State Chem. **88**, 291 (1990).
5. J.-G. Lussier, S.M. Coad, D.F. McMorrow, D. McK Paul, J. Phys. Cond. Matt. **7**, L325 (1995).
6. P.E. Anderson, J.Z. Liu, R.N. Shelton, Phys. Rev. B **56**, 11014 (1997).
7. M. Hase, N. Koide, K. Manabe, Y. Sasago, K. Uchinokura, A. Sawa, Physica B **215**, 164 (1995).
8. M. Hase, K. Uchinokura, R.J. Birgeneau, K. Hirota, G. Shirane, J. Phys. Soc. Jpn **65**, 1392 (1996).
9. M.C. Martin, M. Hase, K. Hirota, G. Shirane, Phys. Rev. B **56**, 3173 (1997).
10. B. Grenier, J.P. Renard, P. Veillet, C. Paulsen, R. Calemcsuk, G. Dhalenne, A. Revcolevschi, Phys. Rev. B **57**, 3444 (1998).
11. M. Saint-Paul, J. Voiron, C. Paulsen, P. Monceau, G. Dhalenne, A. Revcolevschi, J. Phys. Cond. Matt. **10**, 10215 (1998).
12. T. Masuda, A. Fujioka, Y. Uchiyama, I. Tsukada, K. Uchinokura, Phys. Rev. Lett. **80**, 4566 (1998).
13. J.-P. Renard, K. Le Dang, P. Veillet, G. Dhalenne, A. Revcolevschi, L.P. Regnault, Europhys. Lett. **30**, 475 (1995); L.P. Regnault, J.P. Renard, G. Dhalenne, A. Revcolevschi, Europhys. Lett. **32**, 579 (1995).
14. K. Manabe, H. Ishimoto, N. Koide, Y. Sasago, K. Uchinokura, Phys. Rev. B **58**, R575 (1998).
15. B. Batlogg, S.W. Cheong, L.W. Rupp Jr, Physica B **194-196**, 173 (1994).

16. J.F. DiTusa, S.W. Cheong, J.H. Park, G. Aeppli, C. Broholm, C.T. Chen, Phys. Rev. Lett. **73**, 1857 (1994).
17. K. Kojima, A. Keren, L.P. Lee, G.M. Luke, B. Nachumi, W.D. Wu, Y.J. Uemura, K. Kiyono, S. Miyasaka, H. Takagi, S. Uchida, Phys. Rev. Lett. **74**, 3471 (1995).
18. C. Payen, E. Janod, K. Schoumacker, C.D. Batista, K. Hallberg, A.A. Aligia, Phys. Rev. B **62**, 2998 (2000).
19. C. Dasgupta, S.K. Ma, Phys. Rev. B **22**, 1305 (1980).
20. D.S. Fisher, Phys. Rev. Lett. **69**, 534 (1992); D.S. Fisher, Phys. Rev. B **51**, 6411 (1995).
21. D.S. Fisher, Phys. Rev. B **50**, 3799 (1994).
22. E. Westerberg, A. Furusaki, M. Sigrist, P.A. Lee, Phys. Rev. B **55**, 12578 (1997).
23. R.A. Hyman, K. Yang, R.N. Bhatt, S.M. Girvin, Phys. Rev. Lett. **76**, 839 (1996).
24. R.A. Hyman, K. Yang, Phys. Rev. Lett. **78**, 1783 (1997).
25. C. Monthus, O. Golinelli, Th. Jolicoeur, Phys. Rev. Lett. **79**, 3254 (1997).
26. M. Fabrizio, R. Mélin, Phys. Rev. Lett. **78**, 3382 (1997).
27. M. Fabrizio, R. Mélin, Phys. Rev. B **56**, 5996 (1997).
28. M. Fabrizio, R. Mélin, J. Souletie, Eur. Phys. J. B **10**, 607 (1999).
29. R. Mélin, Eur. Phys. J. B **16**, 261 (2000).
30. A. Dobry, P. Hansen, J. Riera, D. Augier, D. Poilblanc, Phys. Rev. B **60**, 4065 (1999).
31. D. Khomskii, W. Geertsma, M. Mostovoy, Czech. J. Phys. **46** (1996) Suppl S6, LT21 Conference Proceedings.
32. H. Fukuyama, T. Tanimoto, M. Saito, J. Phys. Soc. Jpn **65**, 1182 (1996).
33. M. Mostovoy, D. Khomskii, J. Knoester, Phys. Rev. B **58**, 8190 (1998).
34. M. Laukamp, G.B. Martins, C. Gazza, A.L. Malvezzi, E. Dagotto, P.M. Hansen, A.C. López, J. Riera, Phys. Rev. B **57**, 10755 (1998).
35. P.M. Hansen, J.A. Riera, A. Delia, E. Dagotto, Phys. Rev. B **58**, 6258 (1998).
36. P. Hansen, D. Augier, J. Riera, D. Poilblanc, Phys. Rev. B **61**, 6741 (2000).
37. E. Sørensen, I. Affleck, D. Augier, D. Poilblanc, Phys. Rev. B **58**, R14701 (1998).
38. V. Kiryukin, B. Keimer, J.P. Hill, A. Vigliante, Phys. Rev. Lett. **76**, 4608 (1996).
39. M. Horvatić, Y. Fagot-Revurat, C. Berthier, G. Dhalenne, A. Revcolevschi, Phys. Rev. Lett. **83**, 420 (1999).
40. T. Kennedy, J. Phys. Cond. Matt. **2**, 5737 (1990).
41. M. Hagiwara, K. Katsumata, I. Affleck, B.I. Halperin, J.P. Renard, Phys. Rev. Lett. **65**, 3181 (1990).
42. E.S. Sørensen, I. Affleck, Phys. Rev. B 51, 16115 (1995)
43. I. Affleck, T. Kennedy, E.H. Lieb, H. Tasaki, Phys. Rev. Lett. **59**, 799 (1987); Commun. Math. Phys. **115**, 477 (1988).
44. M. Fabrizio, R. Mélin, J. Phys. C **9**, 10429 (1997).
45. F.W.S. Lima, U.M.S. Costa, M.P. Almeida, J.S. Andrade Jr., Eur. Phys. J. B **17**, 111 (2000).
46. C.D. Batista, K. Hallberg, A.A. Aligia, Phys. Rev. B **60**, R12553 (1999); C.D. Batista, K. Hallberg, A.A. Aligia, Phys. Rev. B **58**, 9248 (1998).
47. T. Sakaguchi, K. Kaskurai, T. Yokoo, J. Akimitsu, J. Phys. Soc. Jpn **65**, 3025 (1996).
48. G. Xu, J.F. DiTusa, T. Ito, K. Oka, H. Takagi, C. Broholm, G. Aeppli, Phys. Rev. B **54**, R6827 (1996).